ELSEVIER

Marine Geology 149 (1998) 17–38

MARINE GEOLOGY
INTERNATIONAL JOURNAL OF MARINE GEOLOGY, GEOCHEMISTRY AND GEOPHYSICS

# Structure and geodynamic evolution of the Central Bransfield Basin (NW Antarctica) from seismic reflection data

María José Prieto [a,*], Miquel Canals [a], Gemma Ercilla [b], Marc de Batist [c]

[a] *UA Geociències Marines CSIC-UB, GRC Geociències Marines, Dpt. d'Estratigrafia i Paleontologia, Universitat de Barcelona, E-08071 Barcelona, Spain*

[b] *UA Geociències Marines CSIC-UB, Dpt. de Geologia Marina i Oceanografia Física, Institut de Ciències del Mar (CSIC), Avda. Joan de Borbó s/n, E-08039 Barcelona, Spain*

[c] *Renard Centre of Marine Geology, University of Ghent, Krijgslaan 281 S8, B-9000 Ghent, Belgium*

Received 29 May 1997; accepted 24 March 1998

**Abstract**

The Bransfield Basin is a young active rift basin located between the northern margin of the Antarctic Peninsula and the South Shetland Islands margin. Deception and Bridgeman islands divide the Bransfield Basin in three subbasins, the western, central and eastern. Specific morpho-tectonic features and sediment fill differentiate each subbasin. The structure and geodynamic evolution of the Central Bransfield Basin, which is in a stage of incipient seafloor spreading, have been investigated in detail from a dense grid of single-channel seismic reflection data. The Central Bransfield Basin is dominated by two families of normal faults which are oriented northeast and northwest. The NE-trending faults define three graben systems that are roughly parallel to the basin axis. In an across-basin direction, the mean trend of this family of faults ranges from N71 (the graben system nearest to the Antarctic Peninsula) over N64 (the intermediate graben system), to N53 (the graben system nearest to the South Shetland Islands). The NW-trending family of faults is responsible for the deepening of the basin from southwest to northeast. Both families of faults define the overall Central Bransfield Basin structure, resulting in a complex division of the basin floor. Additionally, tens of volcanic edifices are located on the basin floor, the larger ones being associated to the NW-trending faults. Interaction of tectonics and sedimentation give place to the differentiation of three tectonostratigraphic units, TU1, TU2 and TU3 (from oldest to youngest). TU1 occupies the southernmost graben system, and it is affected by the NE-trending bounding normal faults. TU2 extends further northwestwards than TU1 and essentially fills the intermediate graben system. TU3 represents a further extension of the sediment infill over most of the Central Bransfield Basin, and marks the initiation of the infill of the northernmost graben system. Faults bounding this graben also determine the straight and abrupt morphology of the South Shetland Islands margin. The observed arrangement of the graben systems and the filling tectonostratigraphic units reveal a migration of extensional tectonics and associated depocentres from the Antarctic Peninsula margin to the South Shetland Island margin. The left-lateral rotation from N71 to N53 in the mean trend of the three successive graben systems could have been produced by the oblique subduction of the Phoenix plate and the effect of the sinistral strike-slip movement of the South Scotia Ridge, 200 km northeastwards of the Central Bransfield Basin. 

*Keywords:* Bransfield Basin; rift basin; seafloor spreading; geodynamic evolution; sedimentary infill; tectonostratigraphic units

* Corresponding author. Tel.: +34 (3) 402-1375; Fax: +34 (3) 402-1340; E-mail: mjose@beagle.geo.ub.es

0025-3227/98/$19.00 
*PII* S0025-3227(98)00038-3

## 1. Introduction

The Bransfield Basin (BB) is a NE-trending elongated basin located between the South Shetland Islands (SSI) and the Pacific margin of the Antarctic Peninsula (AP) (Fig. 1a). It is a back-arc basin formed as a result of complex interactions between convergent (Phoenix [1]/South Shetland Islands) and divergent (South Shetland Islands/Antarctic) plates and microplates, sharing plate borders (South Scotia Ridge), fracture zones (Hero to Shackleton), and spreading centres, both extinct (Phoenix and Scotia) and active (Bransfield) (Fig. 1a). BB is divided into three subbasins, western (WBB), central (CBB) and eastern (EBB) Bransfield basins, which are separated by the highs of Deception and Bridgeman islands, respectively (Fig. 1b). Geological–geophysical studies carried out in BB during the last decade support the idea that BB is an active rift basin (Saunders and Tarney, 1984; Keller et al., 1994; Lawver et al., 1995), with subbasins at incipient spreading (CBB) and pre-spreading (EBB) rifting stages (Gràcia et al., 1996, 1997).

This paper deals with the structure and geodynamic evolution of the Central Bransfield Basin (CBB). While some structural features of CBB are already known (Gamboa and Maldonado, 1990; Henriet et al., 1992; Gràcia et al., 1996; Lawver et al., 1996), they have up to present never been incorporated in a detailed study of the basin's geodynamic evolution. Our study encompasses a recognition of: (i) the structure and topography of the acoustic basement; (ii) the morphosedimentary and structural features of the sedimentary cover; and (iii) the relative ages of the structural elements and sediments associated with them. This paper also investigates the relationships between the tectonovolcanic elements interpreted by Gràcia et al. (1996) and the structural and sedimentary components in CBB, in order to contribute to a better understanding of its geodynamic evolution.

[1] The scientific community active in Western Antarctica marine geological research has agreed to use the name 'Phoenix' for the plate that was being subducted along the AP margin, rather than 'Drake' or 'Aluk'. Phoenix is named after the Phoenix lineations in the West Pacific, where the plate was born in the Jurassic. Note there is no evidence for a separate Phoenix plate now. The final remnant of the Phoenix plate became part of the Antarctic plate 4 Ma or so ago. There is also a distinct Shetland microplate (from 'Antarctic Peninsula Region: Conventions Document', agreed by P.F. Barker and eighteen other scientists).

## 2. Geological setting

The Pacific margin of the AP is at present a passive margin (Barker, 1982), but during the Mesozoic and most of the Cenozoic it was an active margin, characterised by the subduction of the Phoenix oceanic plate under the Antarctic plate (Barker and Lawver, 1988) (Fig. 1a). Oblique subduction ceased progressively from southwest to northeast during the Cenozoic, as a result of successive ridge crest–trench collisions (Herron and Tucholke, 1976; Barker, 1982). At about 4 Ma, spreading at the Antarctic–Phoenix ridge in the segment between Hero and Shackleton fracture zones stopped or decreased to a very slow rate, before the spreading centre reached the trench. At that moment, the Phoenix plate became a part of the Antarctic plate (Barker, 1982). Although spreading stopped, subduction at this segment apparently continued, probably driven in the main by the weight of the subducted slab (Jeffers et al., 1991; Barker and Austin, 1994). According to Barker (1982), the rollback effect associated with this sinking plate induced extensional stresses in the overlying plate causing the opening of BB and the distinction of the Shetland microplate. Such an opening, specially at the EEB, also appears clearly influenced by the left-lateral strike-slip movement characterising the near South Scotia Ridge (SSR) an the Shackleton fracture zone (Fig. 1a) (Gràcia et al., 1996, 1997).

Rifting appears to have started with or shortly after the cessation of seafloor spreading along the Antarctic–Phoenix ridge at 4 Ma (Roach, 1978; Barker and Dalziel, 1983). However, geological and geophysical data are not totally coherent and uncertainties about the age of the basin still remain. Recent volcanic and seismic activity (Forsyth, 1975; Pelayo and Wiens, 1989; Fisk, 1990; Gràcia et al., 1996), high heat flow (Nagihara and Lawver, 1989), a positive magnetic anomaly (Roach, 1978), and a large negative gravity anomaly (Garret, 1990), have been recorded along the axis of CBB, indicating that extension continues to occur (Saunders and Tarney, 1984; Fisk, 1990; Lawver et al., 1995).

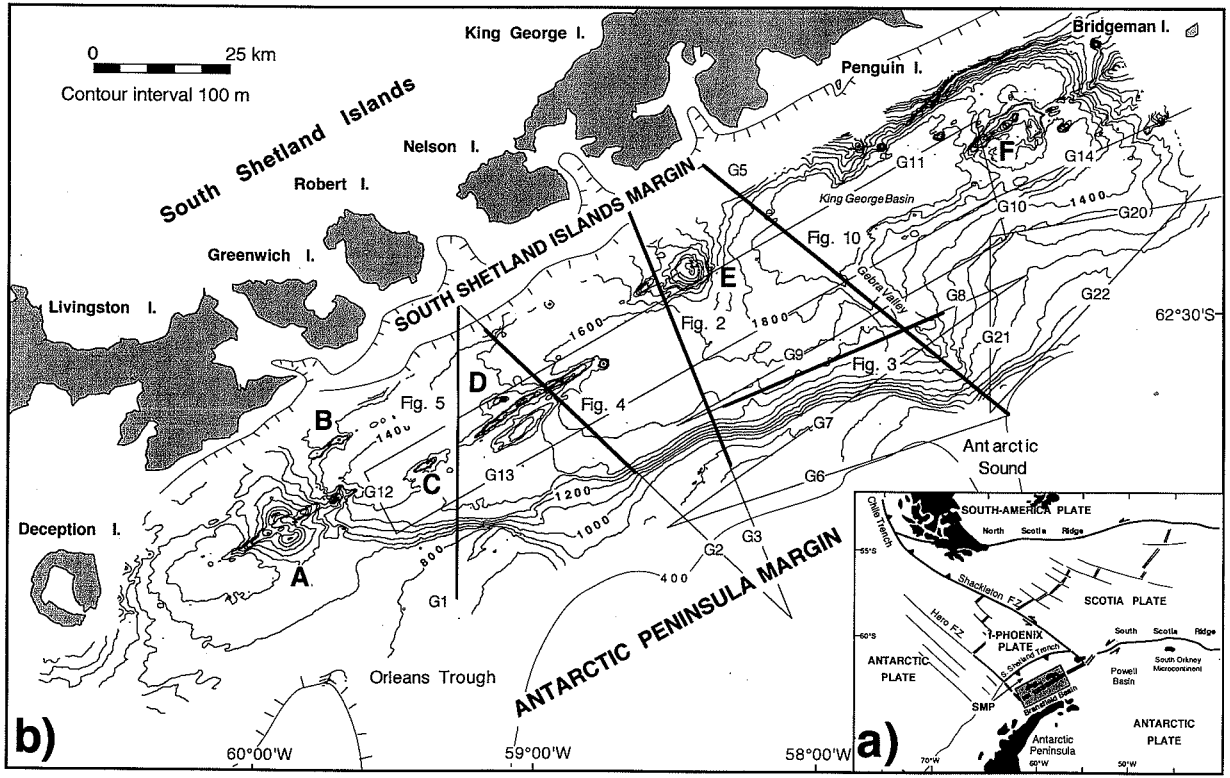


Fig. 1. (a) Geodynamic frame of Bransfield Basin. *SMP* = Shetland microplate. Thin lines show former plate boundaries and fracture zones. Note the sinistral strike-slip movement at the South Scotia Ridge and Shackleton fracture zone. (b) Bathymetric map of the Central Bransfield Basin, with location of seismic lines recorded during the GEBRA '93 cruise. Labels *A* to *F* indicate the location of six large volcanic edifices (modified from Gràcia et al., 1996). Thick lines show location of seismic lines in Figs. 2–5 and 10.

Morphologically, CBB is an asymmetric basin, about 230 km long and 125 km wide, with its SSI and AP margins showing distinct physiography (Fig. 1b). The SSI margin is steep (15–27%), narrow (approx. 5 km wide), rectilinear and is mainly dominated by morphostructural scarps related to extensional faulting (Ashcroft, 1972; Klepeis and Lawver, 1993; Gràcia et al., 1996). The AP margin, on the other hand, is gentler (9 to 15%), wider (approx. 60 km wide) and has an undulating shape in plan view, which is related to the development of prograding sedimentary lobes by glacio-marine processes (Jeffers and Anderson, 1990; Banfield and Anderson, 1995; Prieto et al., 1997). The basin floor separating the AP and SSI margins has a depth ranging from 1000 m in the southwest to 1950 m in the northeast. The along-axis deepening of the basin floor from southwest to northeast takes place through a series of morphological steps separating four main bathymetric levels, as indicated by the swath bathymetry analysis of Gràcia et al. (1996, 1997). They interpret these steps as the surface expression of NW-trending faults.

Associated with these morphological steps, there are six large volcanic edifices (labelled from A to F) which rise above the seafloor (Fig. 1b). They form a discontinuous lineament from Deception Island to Bridgeman Island. This lineament divides the basin floor of CBB into two parts: a southern half-basin, between the AP margin and the volcanic lineament, and a northern half-basin, between the SSI margin and the volcanic lineament (Klepeis and Lawver, 1993). Shapes of the volcanoes vary from circular to elongated, reflecting different tectonovolcanic stages which Gràcia et al. (1996) relate to successive evolutionary stages of basin opening. They observed that both volcanism and tectonic activity have been closely related and preferentially concentrated in the same areas along the CBB axis at certain periods, with evidence of combined extensional faulting and focused active magmatism. Barker and Austin (1994) and Lawver et al. (1995) interpreted the volcanoes in CBB as four parallel zones of linear extrusions resulting from active extension in an extended continental crust that produces linear cracks which leak magma.

Previous seismic reflection investigations of CBB have shown the presence of an acoustic basement, both of igneous and of sedimentary nature, and a sedimentary cover (Gamboa and Maldonado, 1990; Jeffers and Anderson, 1990; Gràcia et al., 1996). The igneous basement has been interpreted as thinned continental crust intruded by dikes and volcanics (Ashcroft, 1972; Guterch et al., 1991; Birkenmajer, 1992). The sedimentary basement is composed of tectonised sedimentary material (Barker and Austin, 1995) which probably corresponds to the Miers Bluff Formation in the SSI margin (Hobbs, 1968; Dalziel, 1969; Smellie et al., 1984) and to the Trinity Peninsula Group in the AP margin (Aitkenhead, 1975; Hyden and Tanner, 1981), which are considered to be correlative (Dalziel, 1984; Storey and Garret, 1985). The sedimentary cover comprises two main sequences separated by a prominent regional unconformity (Gamboa and Maldonado, 1990): a lower 'synrift' sequence, deposited and faulted during the rifting stage, and an upper 'drift' sequence, less tectonised and deposited by glacio-marine sedimentary processes after the main rifting phase (Jeffers and Anderson, 1990).

## 3. Data base and methodology

The data set used in this study was collected during the GEBRA 93 cruise, carried out in December 1993 on board the Spanish R/V *Hespérides*. A total of sixteen lines of single-channel seismic reflection data were recorded in CBB, amounting to about 1100 km (Fig. 1b). The seismic lines are oriented roughly parallel and perpendicular to the basin axis and cover the basin floor and the slopes of the SSI and AP margins. Shots were fired every 5 s using a 2.9 l BOLT airgun operated at 140 bar. The reflected signals were detected with a 150 m long three-channel SIG streamer used in a single-channel configuration. The data were recorded digitally and on-line processed on the high-resolution DELPH2 acquisition system. Post-acquisition data processing, including bandpass filtering, deco-filtering and scaling, was carried out on both the DELPH2 and the PHOENIX VECTOR processing systems.

Seismic data often yield a penetration of 1 s (TWTT) which is generally enough to penetrate the whole sedimentary cover and to recognise the top and part of the acoustic basement. Interpreta-

tion of seismic data has benefited greatly from the new and detailed knowledge of seafloor morphology obtained through swath bathymetric sounding (Gràcia et al., 1996). The bathymetry data helped to determine the presence, orientation and distribution of structures where the seismic data were inconclusive. Morphostructural features identified on the swath bathymetric map, such as scarps, lineaments and abrupt changes of slope, have thus been used to support the structural interpretation.

## 4. Seismic stratigraphy

Our seismic stratigraphic study of CBB has enabled us to define in great detail the seismic features (acoustic character, geometry, stratal patterns) of the basement and sedimentary fill. The acoustic basement shows different seismic facies which have distinct distribution. We attribute the basement composed of massive chaotic facies with reflections of high amplitude, and which appears on the central basin floor between 2 and 3.3 s depth, to crystalline and/or volcanic rocks, in accordance with interpretations of González-Ferrán (1991), Acosta et al. (1992) and Barker and Austin (1994) (Fig. 2). Where the acoustic basement is composed of stratified facies with relatively continuous reflections of medium amplitude, as in the SSI and AP margins down to 1 to 2 s depth, we interpret it as being of sedimentary or metasedimentary nature (Gamboa and Maldonado, 1990; Barker and Austin, 1995).

The sedimentary infill has a variable thickness, ranging from 0.2 s in the SSI margin, to 0.6 s in the AP margin, and to 1 s at the basin floor (Fig. 2). A regional erosional unconformity separates two major sedimentary sequences, the Lower and Upper Sequences, within this infill (Figs. 2 and 3). The deposits of the Lower Sequence are characterised by subparallel, divergent stratified and semitransparent facies with reflections of low lateral continuity and medium to high amplitude that downlap the basement (Fig. 3). The Lower Sequence occurs in the AP margin where it fills and smoothens basement irregularities (Fig. 2). The thickness of this sequence varies from 0.15 to 0.3 s, and the main depocentre (0.3 s) is located below the present AP distal margin. The Upper Sequence is better developed and extends throughout both margins and the basin floor, being partially interrupted by the volcanic lineaments (Fig. 4). Seismically, it is characterised by packages of stratified reflections with high lateral continuity and low to high amplitude that show an oblique configuration in the margins changing to a parallel configuration towards the basin floor. Locally, this facies is interrupted by mound-shaped bodies composed of chaotic facies. The packages of the Upper Sequence display a progradational growth pattern in the SSI and AP margins, and an aggradational pattern on the basin floor (Fig. 5). The thickness of the Upper Sequence ranges from 0.2 s in the SSI margin, over 0.4 s in the AP margin to 1.2 s in the basin floor.

## 5. Structure of the Central Bransfield Basin

The main tectonic features that we identified on CBB are extensional structures. We interpret them to be responsible for the present configuration and structure of the basin. Although much less abundant, we also observed some compressional structures.

### *5.1. Extensional structures*

Extensional structures consist of normal faults bounding graben systems. These faults, which appear to have been active continuously during the evolution of CBB, have a wide spatial distribution (Fig. 6). Two main sets of normal faults can be recognised: NE-trending faults, ranging in orientation from 50°N to 75°N, and NW-trending faults, ranging from 135°N to 165°N (Fig. 6). The NE-trending faults are by far the most numerous. They coincide with the main basin trend and determine the overall basin geometry. NW-trending faults, much less abundant, are practically normal to the basin axis (Fig. 6).

The NE-trending faults are distributed throughout both margins and the basin floor (Fig. 6). These faults affect the acoustic basement and the whole sedimentary cover in the SSI margin (Upper Sequence), and the acoustic basement and Lower Sequence in the AP margin (Fig. 2). At the margins, the NE-trending faults, which have vertical offsets ranging from 0.25 to 1.5 s, deepen the acoustic basement basinward producing a step-like morphology.

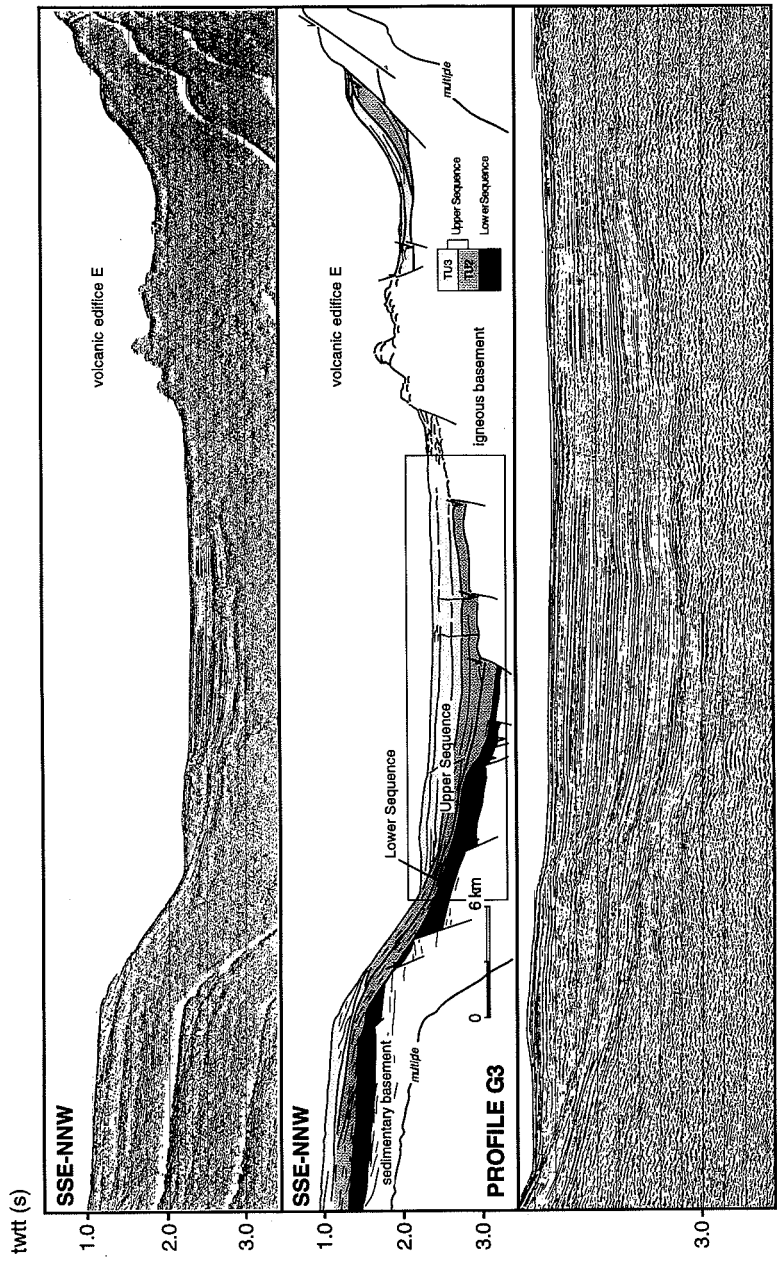


Fig. 2. Seismic line G3, line drawing and detail showing the distribution of the seismic units in the basin and the structures that form the graben systems on both sides of the volcanic edifice E. Shading refers to different tectonostratigraphic units (see discussion in text). Location of seismic line in Fig. 1b.

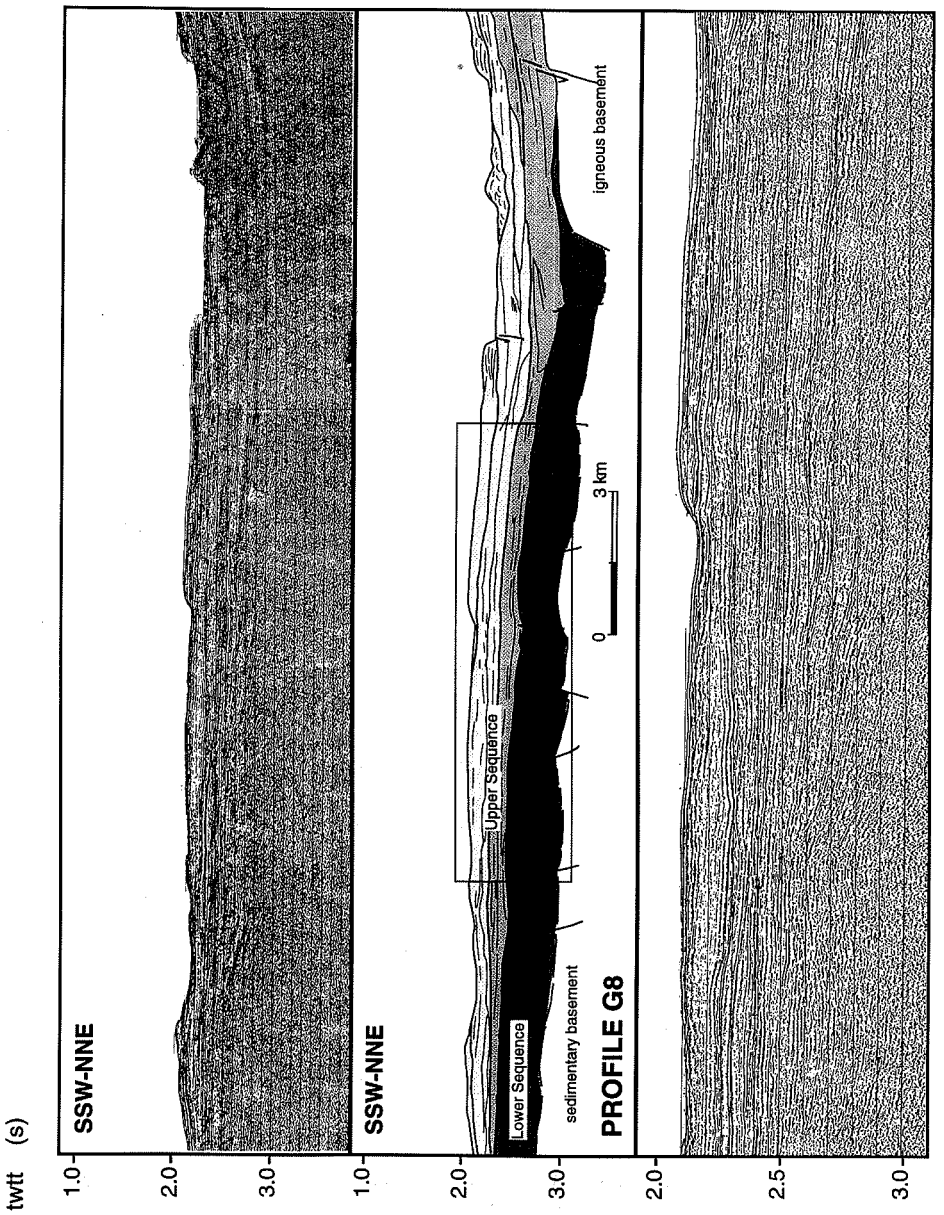


Fig. 3. Seismic line G8, line drawing and detail showing the Lower Sequence, faulted and deformed, and the Upper Sequence, both separated by a strong erosional unconformity. Shading (same legend as Fig. 2) refers to different tectonostratigraphic units (see discussion in text). Location of seismic line in Fig. 1b.

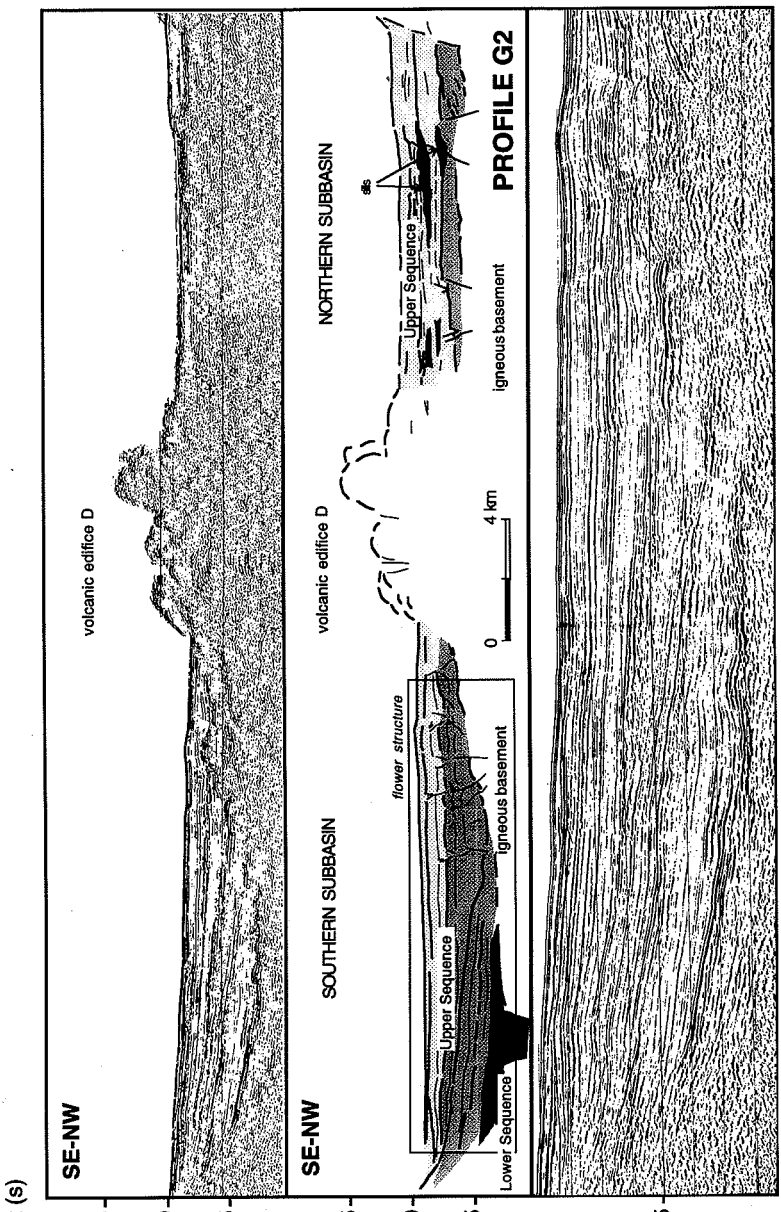


Fig. 4. Seismic line G2, line drawing and detail showing the distribution of basinal seismic units. The volcanic edifice D separates the basin floor into a northern and a southern subbasin. In the southern subbasin a flower structure affects the basement and the Upper Sequence. Shading (same legend as Fig. 2) refers to different tectonostratigraphic units (see discussion in text). Location of seismic line in Fig. 1b.

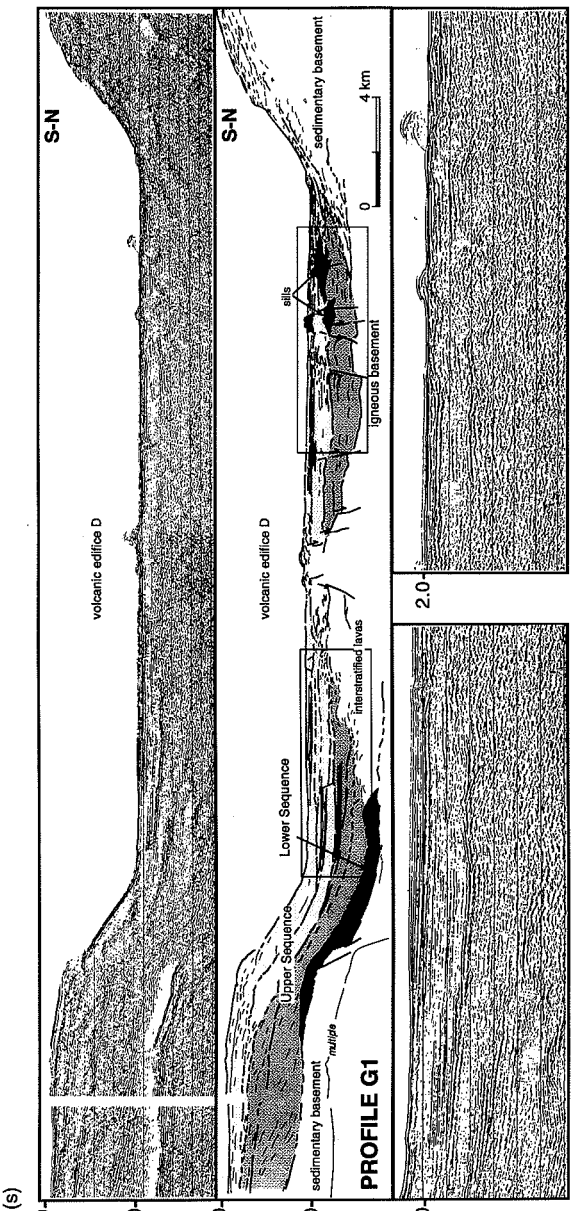


Fig. 5. Seismic line G1, line drawing and details showing the distribution of the Lower and the Upper Sequences. In the southern subbasin sediments are distally interrupted by volcanic layers of volcanic edifice D. In the northern subbasin, bodies with chaotic high-reflective seismic facies have been interpreted as volcanic intrusions/layers associated with normal faults affecting TU3. Shading (same legend as Fig. 2) refers to different tectonostratigraphic units (see discussion in text). Location of seismic line in Fig. 1b.

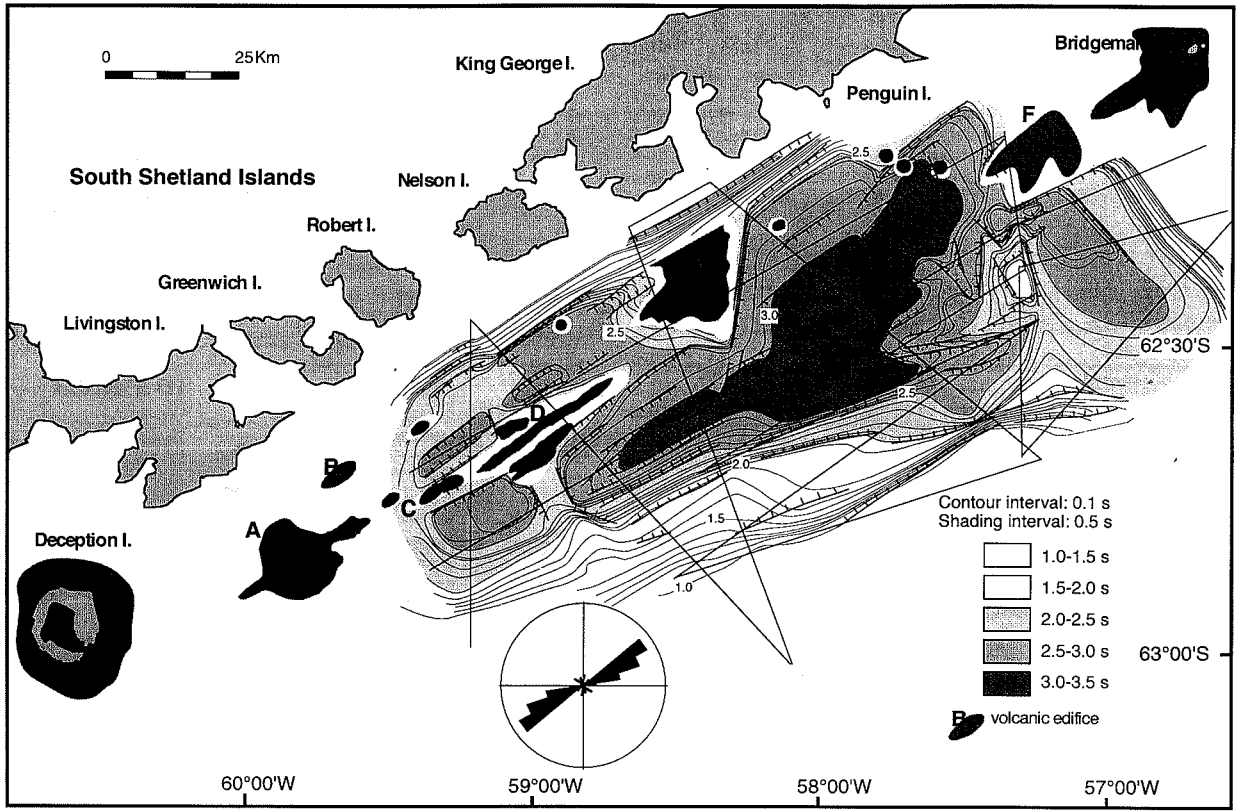


Fig. 6. Isobath map of the acoustic basement and main normal faults affecting it. The circular histogram shows the dominant trends of the fault population, whose mean is N59. Two structural sectors can be distinguished: southwest, between volcanoes A and E, and northeast, between volcanoes E and F.

Basement morphology is not equally reflected in the bathymetry of both margins. In the SSI margin, the step-like morphology is apparent with scarps of 1200 m high and with a gradient of 27% steep, whereas in the AP margin the morphology is smoothened and obliterated by the sedimentary cover (Upper Sequence) (Fig. 1b and Figs. 2 and 3).

Based on the spatial distribution and arrangement of NE-trending faults, two sectors can be distinguished on the basin floor: (i) southwest (between volcanoes A and E); and (ii) northeast (between volcanoes E and F) (Fig. 6). In the southwest sector, the NE-trending faults can be identified on both sides of the volcanoes C, D and E. Immediately south of these three volcanoes, the NE-trending normal faults affect the acoustic basement, deepening it landward with vertical offsets of about 0.25 s (Fig. 2). These faults converge in depth with those identified in the AP margin, forming a narrow NE-trending graben about 5 km wide and 65 km long (Figs. 2 and 6). Faulting and complexity of this graben increase towards the northeast (Fig. 6). North of volcanoes C, D and E, the normal faults affect the acoustic basement and sedimentary cover (i.e. Upper Sequence). They have both basinward and landward polarity and small vertical offsets of about 0.05 s (Figs. 4 and 5). The arrangement of these faults is not as regular as in the southern part. They form a graben about 3 km wide and 35 km long, which is interrupted towards the northeast by volcano E (Figs. 4 and 6).

In the northeast sector of the CBB, the NE-trending faults on the basin floor are located between the volcanic edifices E and F and the AP distal margin (Fig. 6). The faults affect the acoustic basement and the Lower and the Upper Sequences, displaying both landward and basinward polarities, and mean vertical offsets of about 0.05 s. The spatial distribution of these faults, which is more complex than in the southwest sector, shows a radial arrangement with orientations ranging between N50 and N75, converging towards the southwest (Fig. 6). These faults combine and form three almost parallel graben systems of 6 to 10 km wide and 30 to 40 km long (Fig. 7). The geometry of the two southernmost grabens is mostly obliterated by the deposits of the AP margin (Lower and Upper Sequences). In contrast, the geometry of the northernmost graben is reflected in the basin floor bathymetry, which shows a 20 km wide flat trough that corresponds to the King George Basin (1950 m water depth) (Fig. 1b).

Although they are also present in the distal part of the AP margin, the NW-trending faults are concentrated in the basin floor, mainly in the King George Basin (Fig. 6). They mostly affect the acoustic basement, but locally also the Lower and Upper Sequences. These faults show throws of up to 0.3 s, and deepen the acoustic basement towards the King George Basin, intersecting the NE-trending grabens (Fig. 6). The NE and NW structural fragmentation apparently conditioned the complex division of the seafloor and the development of the 1000 m to 1400 m deep platforms in the AP margin.

### *5.2. Compressional structures*

Compressional structures, mostly reverse faults, are much less abundant. In contrast with the extensional structures, reverse faults do not seem to show any preferential orientation. They mostly occur scattered around the volcanic edifices D and E (e.g. Fig. 4). These faults, with vertical offsets between 0.05 and 0.1 s, affect the acoustic basement and the Lower and Upper Sequences, some of them reaching the seafloor where they produce small topographical features of a few metres. Some of these faults branch upward and form small flower structures within the Lower and Upper Sequences (Fig. 4).

## 6. Tectonostratigraphic evolution

The main structural elements described above not only determine the structural framework of CBB but also its depositional trends. The spatial distribution of the structural elements and the different geometries displayed by the deposits of the Lower and Upper Sequences filling the basin have enabled us to define three tectonostratigraphic units: TU1, TU2, and TU3 (from oldest to youngest). The spatial and temporal development of these units reflects changes in the structural configuration, tectonic activity and displacement of sedimentary depocentres within CBB (Fig. 7). We thus use the term 'tectonostratigraphic unit' for seismic stratigraphic units that are not only defined from seismic stratigraphic criteria but also from the tectonic control over their development.

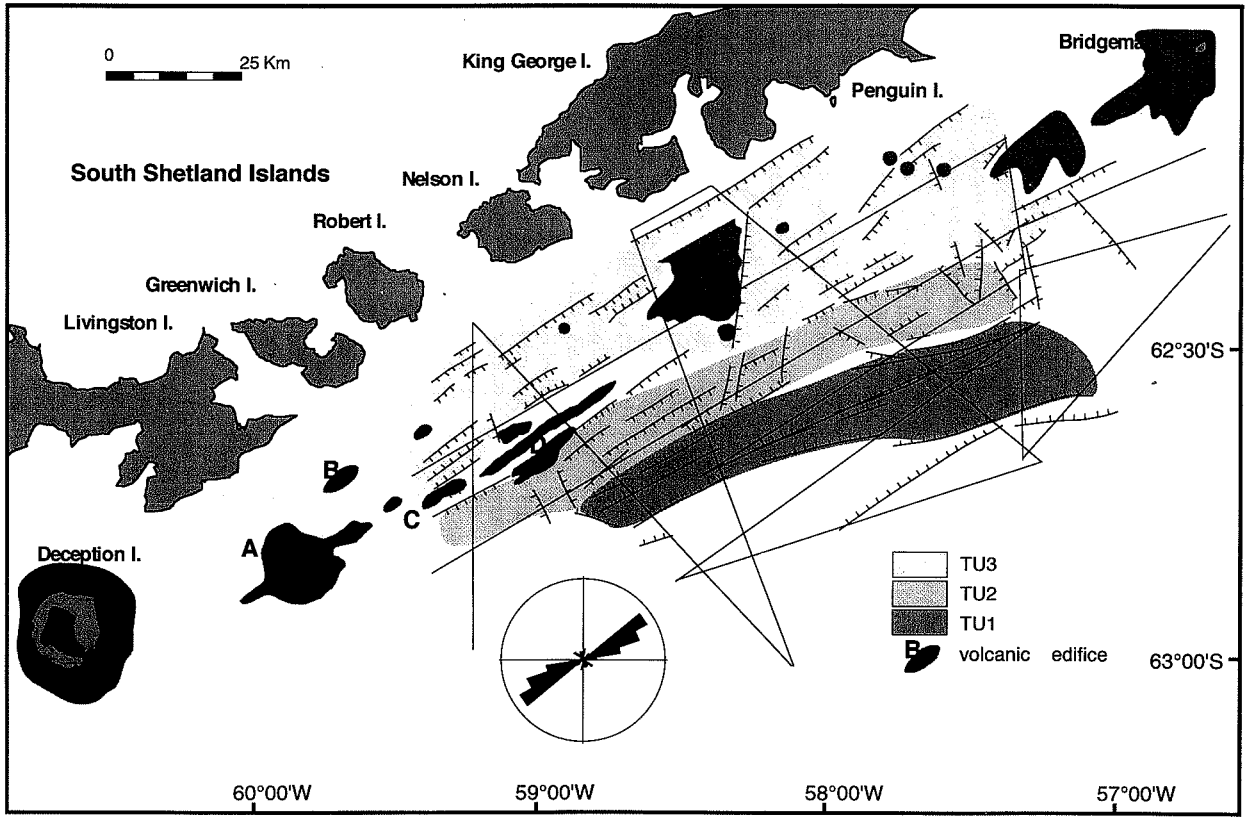


Fig. 7. Cartographic sketch with distribution of main normal faults in CBB and the three resulting graben systems. Shading (same legend as Fig. 2) refers to the tectonostratigraphic units that initially fill each graben (see discussion in text).

### 6.1. Tectonostratigraphic Unit 1 (TU1)

TU1 is located on the AP margin. The deposits of this unit correspond to those of the Lower Sequence, and form a wedge of stratified sediments that onlaps the basement in onshore direction and downlaps onto it towards the offshore (Fig. 5). The upper boundary of TU1 is a strong erosional surface, which is especially prominent at the foot of the AP margin (Fig. 3). In fact, this boundary correlates with the erosional unconformity that separates the Lower and Upper Sequences. Locally, the stratified deposits of TU1 are interrupted in basinward direction by mound-like bodies of chaotic facies, which probably correspond to volcanic flows or laccoliths associated with volcano D (Fig. 5). We have not been able to determine whether TU1 is also present on the SSI margin. Here, a 0.25 s thick wedge of stratified facies downlaps the acoustic basement, but the lack of lateral continuity with TU1 on the AP margin prevents us from establishing whether they were deposited simultaneously, or whether this wedge is younger than TU1 (i.e. TU2) (Fig. 5).

The structural framework of CBB during the development of TU1 is defined by the NE-trending graben system identified along the southwest (between volcanoes A and E) and northeast (between volcanoes E and F) structural sectors (Fig. 6). Normal faults affecting TU1 have a mean trend of N71. During deposition of this unit, tectonic activity was intense (Fig. 8). This is suggested by the presence of numerous faults, stratal pattern and depositional trends (Figs. 2, 3 and 8). Both NE-trending normal faults with throws ranging from 0.25 to 0.5 s, and NW-trending normal faults with throws from 0.1 to 0.2 s, entirely or partially affect the deposits of this unit. The activity of these faults conditioned the general stratal pattern within this unit which shows a subparallel and divergent configuration related to the deepening of the acoustic basement (Fig. 3). Locally, the deposits are landward dipping due to the rotation of the acoustic basement faulted blocks (Fig. 2). The depositional trend of TU1 also reflects the structural control during deposition. The isopach map of this unit, which is up to 0.25 s thick, displays an overall elongated NE-trending pattern. The lateral distribution is locally interrupted by basement highs associated with NW-trending faults (Fig. 8). These interruptions lead to the development of at least four isolated depocentres. The thickness of the deposits within these depocentres increases towards the northeast, from 0.3 to 0.5 s, reflecting a greater deepening of the basement towards this direction (Fig. 8).

At the end of deposition of TU1, tectonic activity in the AP margin of CBB appears to have almost ceased. We infer this from the fact that the NE-trending graben is practically filled up by sediments, which cause the smoothing of pre-existing topographic features and an upward attenuation of the NE- and NW-trending fault offsets (Fig. 3).

### 6.2. Tectonostratigraphic Unit 2 (TU2)

TU2 is located between the AP margin and the axial volcanic lineament, on the southwest and northwest structural sectors, and between the SSI margin and the volcanic lineament on the southwest structural sector (Figs. 7 and 9). The deposits of this tectonostratigraphic unit (0.4 s thick) correspond to the lower section of the Upper Sequence, and are composed of packages of stratified facies that onlap TU1 on the margins and downlap the acoustic basement on the basin floor (Figs. 2, 5 and 10). The stacking of these deposits displays a progradational growth pattern in the margin and an aggradational pattern in the basin floor area (Figs. 2 and 5). The upper boundary of TU2 is a conformable surface. As occurs with TU1, the deposits of TU2 are distally interrupted by highly reflective chaotic bodies which we interpreted as volcanic layers probably associated with volcanic edifice D (Fig. 5). The top of TU2 marks a sharp reduction in the presence of volcanic material in the southwest sector, especially to the south of the volcanic lineament (Fig. 5).

The structural framework of CBB during the formation of TU2 is characterised by a graben system located immediately north of the one filled by TU1 (Fig. 7). During deposition of TU2, synsedimentary deformation is less important than in TU1 times, and mainly affects the southwest sector of CBB (Fig. 9), where TU2 is cut by NE-trending normal faults with vertical offsets ranging from 0.05 to 0.1 s, and by NW-trending faults with 0.05 s of vertical offset. Reverse faults with vertical offsets <0.05 s and flower structures around the volcanoes also occur (Fig. 4). Normal faults affecting TU2 have a mean trend of

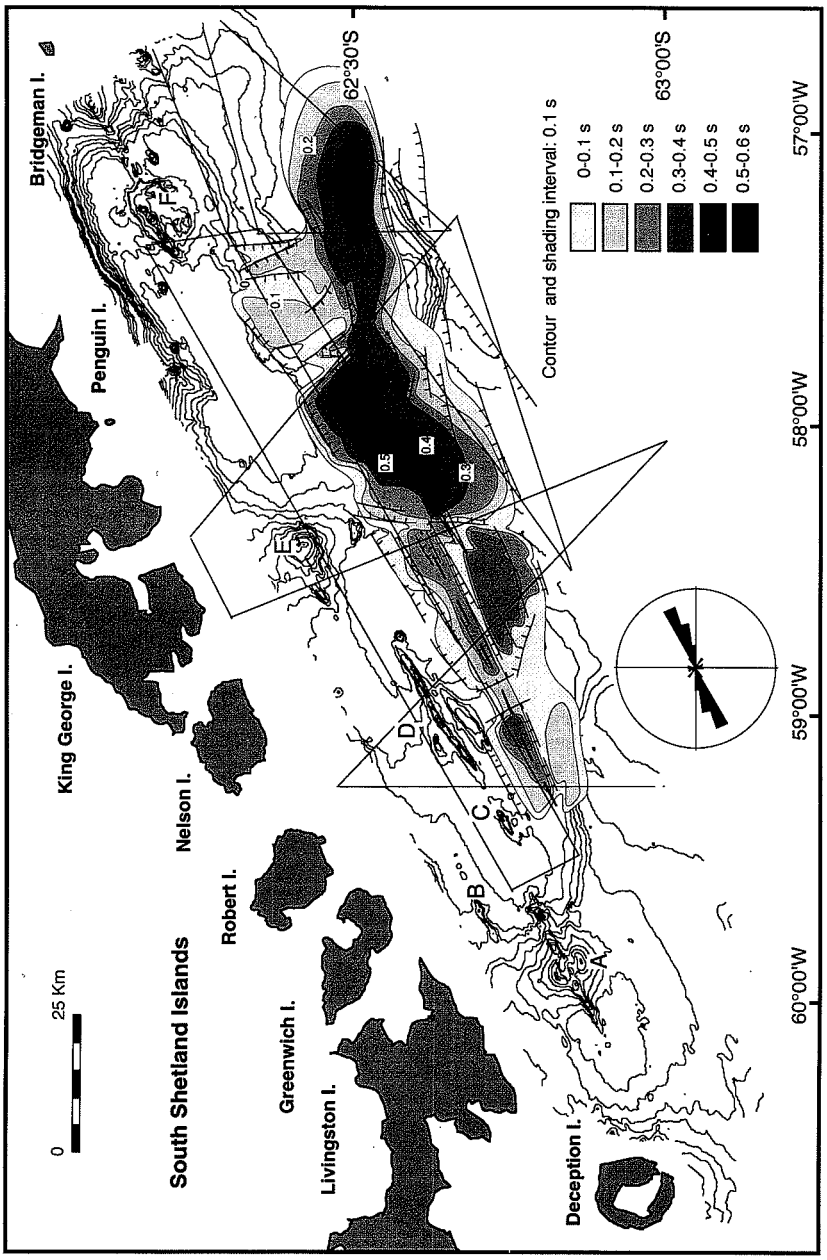


Fig. 8. Isopach map of TU1 and main normal faults affecting it. The circular histogram shows the dominant trend of these faults, whose mean is N71. Discontinuous thick lines mark the position of depocentres. For values of bathymetry contours, see Fig. 1b.

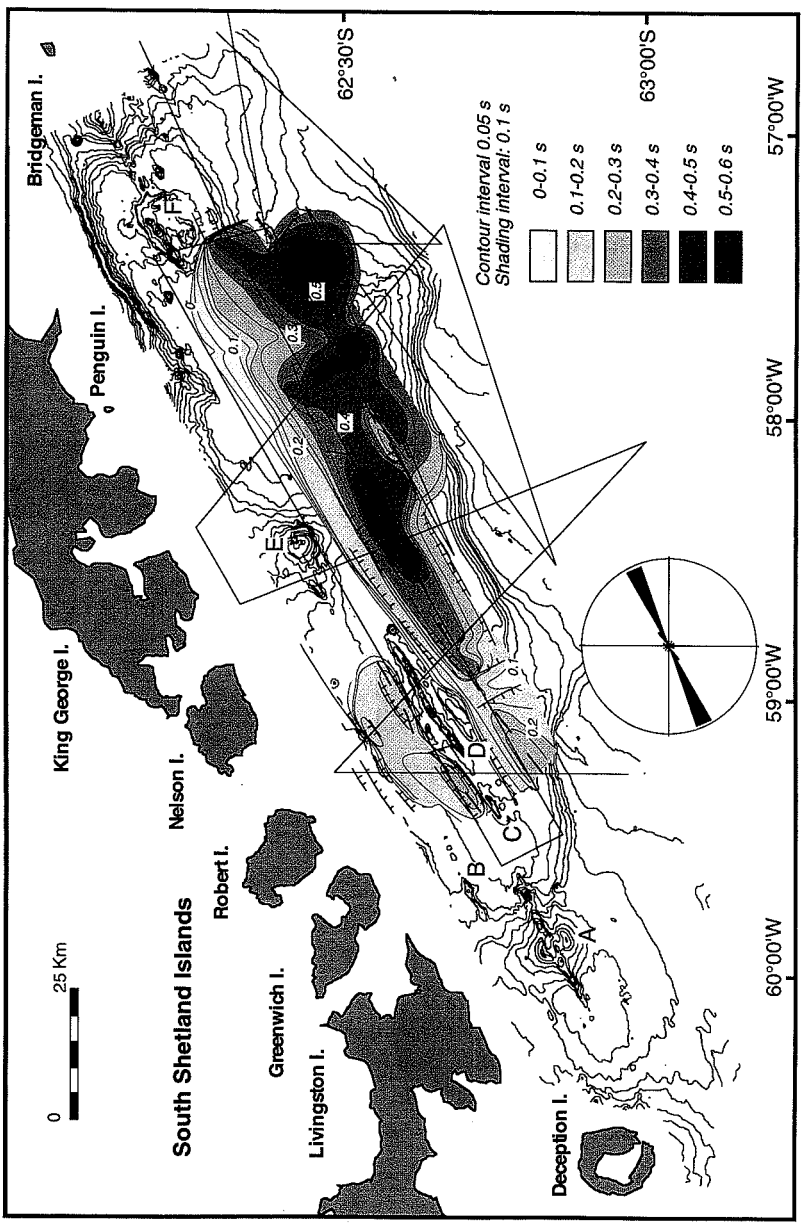


Fig. 9. Isopach map of TU2 and main normal faults affecting it. The circular histogram shows the dominant trend of these faults, whose mean is N64. Discontinuous thick lines mark the position of depocentres. For values of bathymetry contours, see Fig. 1b.

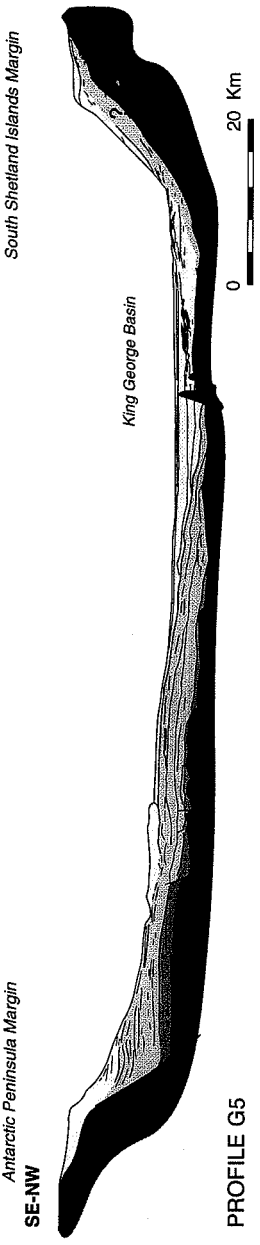


Fig. 10. Interpretative sketch of line G5, showing the distribution of tectonostratigraphic units TU1, TU2 and TU3. *Bt* = acoustic basement, either sedimentary or igneous; *V* = volcanics; *TU1*, *TU2*, *TU3* = tectonostratigraphic units. Question mark indicates that this sedimentary body could also correspond to TU1. Location of seismic line in Fig. 1b.

N64 (Fig. 9). The northeast sector lacks significant faulting, and the two main depocentres are not coincident with the structural regional trends. The shapes of these depocentres range from roughly semicircular (0.5 s thick) to elongated in a NW direction (0.6 s thick), which reflect the effect of the uneven sediment supply coming from the AP margin in TU2 (Fig. 9).

Nevertheless, the structural frameworks have had a significant influence on the overall distribution of sediments in TU2. The isopach map shows how the isoline directions and depocentre axes in the southwest sector follow a NE direction, and also show the sharp influence of the axial volcanic lineament separating two depocentres to the northwest (Fig. 9). The organisation of the sedimentary depocentres in TU2 is also conditioned by the activity of the NW-trending faults and rare N-trending faults (Fig. 9).

### 6.3. Tectonostratigraphic Unit 3 (TU3)

TU3 marks the shift from sedimentation restricted to the marginal areas and isolated basinal depocentres, to deposition occurring throughout CBB (Fig. 7). During TU3 times the present-day structural framework is achieved. TU3 comprises the uppermost deposits (0.4 s thick) of the Upper Sequence. Seismically, TU3 is similar to TU2, and it is also formed by packages of stratified deposits which onlap TU2 sediments and the acoustic basement, both on the margins and basin floor (Figs. 2, 4, 5 and 10). The growth pattern of this unit is progradational in the margins, changing to aggradational on the basin floor. Locally, the stratified facies contains reflections of higher acoustic amplitude (Figs. 4 and 5). We interpret these as volcanic layers associated with volcanoes D, E and probably also with other small volcanic cones located between the axial volcanic lineament and the SSI margin (Fig. 1b).

The structural framework of CBB during TU3 is characterised by the development of a graben system north of that which developed during deposition of TU2 and whose influence is still apparent (Fig. 7). During TU3 times synsedimentary deformation becomes more significant than in TU2 times, and it mainly affects the deposits on the SSI margin and on the basin floor north of the volcanic lineament defined by volcanoes C, D and E (Fig. 11). There, numerous faults occur as well as slightly deformed deposits. Normal faults affecting TU3 have a mean trend of N53. The structures include NE-trending normal faults with offsets around 0.05 s (Figs. 2, 4 and 5) and much less important, reverse faults (with offsets <0.05 s) and flower structures that are always located near the volcanic edifices (Fig. 4). The NE-trending faults produce scarps that are reflected in the bathymetry of the SSI margin and that may reach up to 1200 m of relief (Fig. 1b). These scarps are sediment covered on slope locations as seen in Fig. 10.

During TU3 times there is a clear structural control on sediment distribution in the SSI margin, the basin floor north of the volcanic lineament defined by volcanoes C, D and E (Figs. 2, 4 and 5) and King George Basin (Fig. 11). In contrast, on the AP margin sedimentation is essentially governed by the sediment input (either from point or linear sources) and glacio-marine sedimentation processes. The isopach map shows three main depocentres of 0.35, 0.4 and 0.45 s of thickness (Fig. 11). The two main depocentres coincide with the new northern graben system, whereas the smallest one appears to have developed along structures inherited from TU2. Such a sedimentary influence is highlighted by the sinuosity of the isolines, which locally follow directions that are occasionally perpendicular to the margin (Fig. 11).

## 7. Discussion

The sediment infill of CBB is usually described as being composed of two main seismic stratigraphic units, the Lower Sequence and the Upper Sequence, that are interpreted as synrift and postrift depositional units, respectively (Gamboa and Maldonado, 1990; Jeffers and Anderson, 1990; Prieto et al., 1997). In this study, we have been able to further subdivide these two main seismic stratigraphic sequences into three unconformity-bounded tectonostratigraphic units: TU1, TU2 and TU3, where TU1 is the Lower Sequence and TU2 and TU3 constitute the Upper Sequence. Deposition of TU1 was induced by the initial fragmentation of the continental crust of AP which favoured sediment accumulation over graben systems and tilted blocks now beneath the slope of the AP margin (Figs. 2 and 3). The

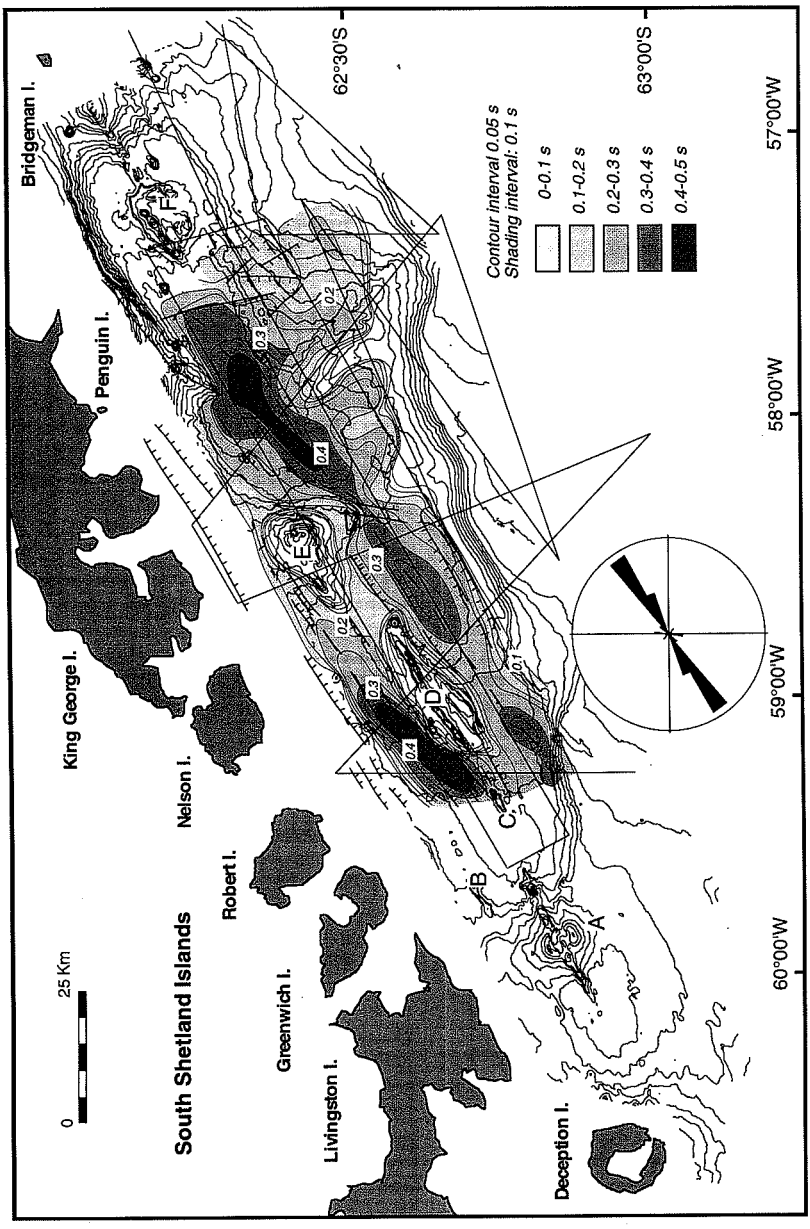


Fig. 11. Isopach map of TU3 and main normal faults affecting it. The circular histogram shows the dominant trend of these faults, whose mean is N53. The bathymetric contouring overlays isopach map to make visible how TU3 fits present-day bathymetry. Discontinuous thick lines mark the position of depocentres. For values of bathymetry contours, see Fig. 1b.

upper boundary is a regional truncation that could be interpreted as the break-up unconformity, which would separate rift from drift sequences (Gamboa and Maldonado, 1990; Jeffers and Anderson, 1990).

Structural deformation along normal faults suggests a strong interaction between sedimentation and extensional tectonism throughout the history of CBB. Structurally controlled depocentres govern the temporal and spatial distribution of the tectonostratigraphic units, which successively fill younger NE-elongated graben systems (Fig. 7). Seismic profiles and resulting isoline maps derived from them reveal a parallel across-basin axis migration (SE–NW direction) of the graben systems and TUs' depocentres from the AP margin to the SSI margin. Faults affecting the basement and TU1 attenuate upwards and only few of them also affect TU2 (Figs. 2 and 3). The same is valid for normal faults within TU2 and their continuation into TU3. The most recent faults affecting TU3 are concentrated near the SSI margin, some of them being inherited from former episodes (Fig. 11). Migration of the tectonic activity (deformation) also favours the asymmetric structure of CBB as showed by the contrasting physiography between the AP and SSI margins. Smoothened relief at the AP margin results from sustained glaciomarine sedimentation since the earliest opening of CBB. Dramatic relief of the straight SSI margin and the young sediment cover witnesses the youth of this part of CBB. Limited sediment input on the SSI margin is also related to the smaller ice-shed area of the archipelago compared to that of the AP.

Interaction between sedimentation and volcanism is revealed by the barrier effect of volcanic lineaments at the time of deposition of each tectonostratigraphic unit (Figs. 8 and 9), by interstratified layers of probable volcanic origin, and by sills intruded into the sediments (Figs. 4 and 5). The axial volcanic lineaments were more effective in preventing an homogeneous distribution of sediments, with the development of separated depocentres during deposition of TU2 (Fig. 9). However, a specific point regards the formation of the King George Basin. Since there is no structural barrier, neither volcanic nor of any other nature, impeding the dispersion of TU2 sediments, comparison of isopach maps on Figs. 9 and 11 suggests that the King George Basin was mostly formed after sedimentation of TU2, during the tectonic phase that caused the depocentre shift from TU2 to TU3.

The distribution, configuration and tectonic influence of the three TUs allow the reconstruction of the opening history of CBB, which started very close to the present-day AP margin and propagated to the northwest, towards the SSI margin. The opening of CBB apparently occurred in three distinct phases corresponding to the three main episodes of the depositional history: TU1, TU2 and TU3. During the first phase, a narrow graben was formed near AP (Fig. 7). This graben was filled by TU1 sediments (Fig. 8). Segments of the main volcanic lineament were developed during deposition of TU1, as suggested by the isopach map of TU1 and by the fact that their deposits pinch out against and downlap onto the southern ridge of volcano D (Figs. 5 and 8). Gràcia et al. (1996) already postulated, based on morphological criteria, that the lateral ridges of volcano D could be the oldest volcanic features in CBB. During the second phase, volcanic activity and growth of the volcanic ridge followed, with continued and renewed extension. At the same time TU2 accumulated in the newly created space, as suggested by volcanic layers intercalated within TU2 sediments (Fig. 5). During the third phase the main locus of extension shifted further to the northwest, towards the SSI margin, where it seems still active at present (Fig. 7). It is during this phase that the present configuration of CBB was obtained, as revealed by the fact that only TU3 occurs all over CBB (Fig. 11). New volcanoes, i.e. volcanoes E and F, were formed or substantially grew, while older ones continued their growth. Quaternary volcanism recorded at Deception, Penguin and Bridgeman islands (Fig. 1b) (Weaver et al., 1979), and high heat flow values typical of regions with active hydrothermal circulation (Nagihara and Lawver, 1989; Lawver et al., 1995), support the idea of an active volcanism in CBB. Furthermore fresh and glassy basalts less than 100,000 years old have been also recovered from the volcanic edifice F (Fisk, 1990).

The roll-back induced by the continued sinking and subduction of the Phoenix plate under the Shetland microplate (Barker, 1982; Barker and Dalziel, 1983; Barker et al., 1988) could have caused continued extension in CBB and migration of the tectonically active bands and depocentres from the AP

margin to the SSI margin. Lateral displacement and interruptions, of what otherwise would have been a continuous, elongated and unique depocentre for each tectonostratigraphic unit, suggest NW-guided tectonic displacements which we attribute to the NW-trending faults (Figs. 7–9 and 11). Gràcia et al. (1996, 1997) identified the same structural direction in NW-trending bathymetric steps and related it to a sort of inherited prolongation of the fracture zones on the Phoenix plate. The NW structural direction has been also recognised in the two main islands bordering CBB, Livingston (Pallàs et al., 1995) and King George (Tokarski, 1991).

Another aspect to be noted, concerning the geodynamics of CBB, is the left-lateral rotation of the dominant fault trend from one phase to the next one: N71 for TU1, N64 for TU2 and N53 for TU3. Sinistral strike-slip movement at the South Scotia Ridge (SSR), together with the oblique subduction of the Phoenix plate, could be responsible for the left-lateral rotation of fault populations from TU1 to TU3. The strike-slip influence of the SSR is particularly apparent in the Eastern Bransfield Basin (EBB) (Klepeis and Lawver, 1996), where various pull-apart basins have been identified by Gràcia et al. (1996, 1997).

Our results raise serious doubts to the interpretation of the unconformity at the top of TU1 as the only break-up unconformity in CBB. Rather than that, the migration history of CBB opening, as we have showed, would indicate that there could not be one single break up unconformity, of synchronic character throughout the basin, but perhaps two of them, separating three tectonic stages in the opening of CBB.

## 8. Conclusions

The strong interaction between glacio-marine sedimentation and extensional tectonism throughout the history of CBB is illustrated by the development of three tectonostratigraphic units (TU1, TU2 and TU3), filling differentiated, fault-controlled depocentres that have migrated towards the northwest, from the AP margin to the SSI margin.

The NW migration of the tectonically active bands and the left-lateral rotation of the dominant fault population trends from TU1 to TU3 (N71 to N53) can be explained by the combined influence of: (i) the roll-back and oblique subduction of the Phoenix plate under the Antarctic plate and the Shetland microplate and; (ii) the sinistral strike-slip movement from the South Scotia Ridge.

The infill of CBB is, at its origin, essentially tectonically driven with the particularity that the tectonic imprint has been progressively replaced by a glacio-marine imprint from southeast (AP margin) to northwest (SSI margin). Volcanism associated to the extension of CBB appeared once the opening of the basin had already progressed substantially and continues to the present day.

## Acknowledgements

We cordially thank the captain of the R/V *Hespérides*, Commandant V. Quiroga, and the crew members who participated in the GEBRA 93 cruise. We thank M. Farrán and J. Sorribas for processing the swath-bathymetry data. We would also like to thank E. Uchupi, J. Woodside, E. Gràcia and the editor, whose comments and suggestions have greatly improved the article. This work was supported by the Spanish 'Programa Nacional de Investigación en la Antártida', project ANT-93-1008-C03-01, funded by the CICYT. The GRC Geociències Marines at the Universitat of Barcelona has been supported by 'Generalitat de Catalunya' grant GRC 94/95-1026. M.J. Prieto benefited from a fellowship from the 'Universitat de Barcelona' (CPI-16), and M. De Batist is senior research assistant of the FWO Vlaanderen. The participation of the University of Ghent (Belgium) in the GEBRA 93 cruise was supported by the Belgian Program of Antarctic Research Programme, project A3-02-002.

## References

Acosta, J., Herranz, P., Sanz, J.L., Uchupi, E., 1992. Antarctic continental margin: geologic image of the Bransfield Trough, an incipient ocean basin. In: Poag, C.W., Graciansky, P.C. (Eds.), Geologic Evolution of Atlantic Continental Rises. Van Nostrand Reinhold, New York, pp. 49–61.

Aitkenhead, N., 1975. The Geology of the Duse Bay–Larsen inlet area, North-East Graham Land (with particular reference

to the Trinity Peninsula Series). BAS Sci. Rep. 51, 62 pp.

Ashcroft, W.A., 1972. Crustal structure of the South Shetland Islands and Bransfield Strait. BAS Sci. Rep. 66, 43 pp.

Banfield, L.A., Anderson, J.B., 1995. Seismic facies investigation of the Late Quaternary glacial history of Bransfield Basin, Antarctica. In: Cooper, A.K., Barker, P.F., Brancolini, G. (Eds.), Geology and Seismic Stratigraphy of the Antarctic Margin. AGU, Antarct. Res. Ser. 68, 123–140.

Barker, D.H.N., Austin, J.A., 1994. Crustal diapirism in Bransfield Strait, West Antarctica. Evidence for distributed extension in marginal basin formation. Geology 22, 657–660.

Barker, D.H.N., Austin, J.A., 1995. Characterization of acoustic basement, Bransfield Strait: implications for geologic evolution of this marginal basin. Abstr. VII ISAES, p. 20.

Barker, P.F., 1982. The Cenozoic subduction history of the Pacific margin of the Antarctic Peninsula: Ridge crest-trench interactions. J. Geol. Soc. London 139, 787–801.

Barker, P.F., Dalziel, I.W.D., 1983. Progress in geodynamics of the Scotia Arc region. In: Cabré, R. (Ed.), Geodynamics of the Eastern Pacific Region, Caribbean and Scotia Arcs. AGU, Geodyn. Ser. 9, 137–170.

Barker, P.F., Lawver, L.A., 1988. South American–Antarctic plate motion over the past 50 Myr, and the evolution of the South American–Antarctic Ridge. Geophys. J. 94, 377–386.

Barker, P.F., Dalziel, I.W.D., Storey, B.C., 1988. Tectonic development of the Scotia Arc region. In: Tingey, R.J. (Ed.), Antarctic Geology. Oxford Univ. Press, Oxford, pp. 215–248.

Birkenmajer, K., 1992. Evolution of the Bransfield Basin and Rift, West Antarctica. In: Yoshida, Y., Kamimura, K., Shiraishi, K. (Eds.), Recent Progress in Antarctica, Earth Science. Terra, Tokyo, pp. 405–410.

Dalziel, I.W.D., 1969. Structural studies in the Scotia Arc: Livingston Island. Antarct. J. U. S. 4, 137.

Dalziel, I.W.D., 1984. Tectonic evolution of a fore-arc terrane, Southern Scotia Ridge, Antarctica. Geol. Soc. Am. Spec. Pap. 200, 32 pp.

Fisk, M.R., 1990. Volcanism in the Bransfield Strait, Antarctica. J. South Am. Earth Sci. 3, 91–101.

Forsyth, D.W., 1975. Fault plane solutions and tectonics of South Atlantic and Scotia Sea. J. Geophys. Res. 80, 1424–1443.

Gamboa, L.A.P., Maldonado, P.R., 1990. Geophysical investigations in the Bransfield Strait and in the Bellingshausen Sea. In: John, B.St. (Ed.), Antarctica as an Exploration Frontier: Hydrocarbon Potential, Geology, and Hazards. Am. Assoc. Pet. Geol. Stud. Geol. 31, 127–142.

Garret, S.W., 1990. Interpretation of reconnaissance gravity and areomagnetic surveys of the Antarctic Peninsula. J. Geophys. Res. 95, 6759–6777.

González-Ferrán, O., 1991. The Bransfield rift and its active volcanism. In: Thomson, M.R.A., Crame, J.A., Thomson, J.W. (Eds.), Geological Evolution of Antarctica. Cambridge Univ. Press, Cambridge, pp. 505–509.

Gràcia, E., Canals, M., Farràn, M., Prieto, M.J., Sorribas, J., Gebra Team, 1996. Morphostructure and evolution of the Central and Eastern Bransfield Basins (NW Antarctic). Mar. Geophys. Res. 18 (1–3), 429–448.

Gràcia, E., Canals, M., Farràn, M., Sorribas, J., Pallàs, R., 1997. The Central and Eastern Bransfield basins (Antarctica) from high-resolution swath-bathimetry data. Antarct. Sci. 9 (2), 168–180.

Guterch, A., Grad, M., Janik, T., Perchuc, E., 1991. Tectonophysical models of the crust between the Antarctic Peninsula and the South Shetland trench. In: Thompson, M.R.A., Crame, J.A., Thomson, J.W. (Eds.), Geological Evolution of Antarctica. Cambridge Univ. Press, Cambridge, pp. 499–504.

Henriet, J.P., Meissner, R., Miller, H., Team, G., 1992. Active margin processes along Antarctic Peninsula. Tectonophysics 201, 1–25.

Herron, E.M., Tucholke, B.E., 1976. Sea floor magnetic patterns and basement structure in the southeastern Pacific. In: Hollister, C.D., Cradock, C. (Eds.), Init. Rep. DSDP. U.S. Government Printing Office, Washington, pp. 263–278.

Hobbs, G.J., 1968. The geology of the South Shetland Islands. IV The Geology of Livingston Island. BAS Sci. Rep., 47, 34 pp.

Hyden, G., Tanner, W.G., 1981. Late Paleozoic–Early Mesozoic fore-arc basin sedimentary rocks at the Pacific Margin in Western Antarctica. Geol. Rundsch. 70, 529–541.

Jeffers, J.D., Anderson, J.B., 1990. Sequence stratigraphy of the Bransfield Basin, Antarctica. Implications for tectonic history and hydrocarbon potential. In: John, B.St. (Ed.), Antarctica as an Exploration Frontier: Hydrocarbon Potential, Geology and Hazards. Am. Assoc. Pet. Geol. Stud. Geol. 31, 13–30.

Jeffers, J.D., Anderson, J.B., Lawver, L.A., 1991. Evolution of the Bransfield basin, Antarctic Peninsula. In: In: Thompson, M.R.A., Crame, J.A., Thomson, J.W. (Eds.), Geological Evolution of Antarctica. Cambridge Univ. Press, Cambridge, pp. 481–485.

Keller, R.A., Strelin, J.A., Lawver, L.A., Fisk, M.R., 1994. Dredging young volcanic rocks in Bransfield Strait. Antarct. J. U. S. XXVIII, (1993 Rev. Iss.), 98–100.

Kepleis, K., Lawver, L., 1993. Bathymetry of the Bransfield Strait, southeastern Shackleton Fracture Zone, and South Shetland Trench, Antarctica. Antarct. J. U. S. XXVIII (No. 5 Rev.), 103–104.

Klepeis, K.A., Lawver, L.A., 1996. Tectonics of the Antarctic–Scotia plate boundary near Elephant and Clarence Islands, West Antarctica. J. Geophys. Res. 101, 20211–20231.

Lawver, L.A., Keller, R.A., Fisk, M.R., Strelin, J., 1995. Bransfield Strait, Antarctic Peninsula: Active extension behind a dead arc. In: Taylor, B. (Ed.), Back-arc Basins: Tectonics and Magmatism. Plenum, New York, pp. 315–342.

Lawver, L.A., Ghidella, M., Von Herzen, R.P., Keller, R., 1996. Distributed, active extension in Bransfield Basin, Antarctic Peninsula: evidence from multibeam bathymetry. GSA Today 6 (11), 1–6.

Nagihara, S., Lawver, L.A., 1989. Heat flow measurements in the King George Basin, Bransfield Strait. Antarct. J. Sci. 23, 123–125.

Pallàs, R., Vilaplana, J.M., Sàbat, F., 1995. Geomorphological and neotectonic features of Hurd Peninsula, Livingston Island, South Shetland Islands. Antarct. Sci. 7 (4), 395–406.

Pelayo, A.M., Wiens, D.A., 1989. Seismotectonics and relative

plate motions in the Scotia Sea region. J. Geophys. Res. 94, 7293–7320.

Prieto, M.J., Gràcia, E., Canals, M., Ercilla, G., De Batist, M., 1997. Sedimentary history of the Central Bransfield Basin (NW Antarctic Peninsula). In: Ricci, C.A. (Ed.), The Antarctic Region: Geological Evolution and Processes. Proc. VII ISAES, Terra Ant., Siena, pp. 711–717.

Roach, P.J., 1978. The nature of back-arc extension in Bransfield Strait. Geophys. J. Res. Astron. Soc. 53, 165.

Saunders, A.D., Tarney, J., 1984. Geochemical characteristics of basaltic volcanism within backarc basins. In: Kokelaar, B.P., Howells, M.F. (Eds.), Marginal Basin Geology: Volcanism and Associated Sedimentary and Tectonic Processes in Modern and Ancient Marginal Basins. Geol. Soc. London Spec. Publ. 16, 59–76.

Smellie, J.L., Pankhurst, R.J., Thomson, M.R.A., Davies, R.E.S., 1984. The Geology of the South Shetland Islands: VI Stratigraphy, Geochemistry and Evolution. BAS Sci. Rep. 87, 85 pp.

Storey, B.C., Garret, S.W., 1985. Crustal growth of the Antarctic Peninsula by accretion, magmatism and extension. Geol. Mag. 122, 15–25.

Tokarski, A.K., 1991. The Late Cretaceous–Cenozoic structural history of King George Island, South Shetland Islands, and its plate-tectonic setting. In: Thomson, M.R.A., Crame, J.A., Thomson, J.W. (Eds.), Geological Evolution of Antarctica. Cambridge Univ. Press, Cambridge, pp. 493–497.

Weaver, S.D., Saunders, A.D., Pankhurst, R.J., Tarney, J., 1979. A geochemical study of magmatism associated with the initial stages of back-arc spreading: the Quaternary volcanics of Bransfield Strait from South Shetland Islands. Contrib. Mineral. Petrol. 68, 151–169.